



Article

Resistance of Grassland under Different Drought Types in the Inner Mongolia Autonomous Region of China

Jian Guo ^{1,2} , Xiuchun Yang ^{3,*}, Weiguo Jiang ^{1,2} , Xiaoyu Xing ³, Min Zhang ³, Ang Chen ³, Dong Yang ³, Mingxin Yang ³, Lunda Wei ³ and Bin Xu ⁴

¹ State Key Laboratory of Remote Sensing Science, Faculty of Geographical Science, Beijing Normal University, Beijing 100875, China; guojian@bnu.edu.cn (J.G.); jiangweiguo@bnu.edu.cn (W.J.)

² Beijing Key Laboratory for Remote Sensing of Environment and Digital Cities, Faculty of Geographical Science, Beijing Normal University, Beijing 100875, China

³ School of Grassland Science, Beijing Forestry University, Beijing 100083, China; xingxiaoyu@bjfu.edu.cn (X.X.); zhangmin_rs@bjfu.edu.cn (M.Z.); chenang0226@bjfu.edu.cn (A.C.); yd96062@bjfu.edu.cn (D.Y.); ymxin@bjfu.edu.cn (M.Y.); wld0908@bjfu.edu.cn (L.W.)

⁴ Key Laboratory of Agri-Informatics, Ministry of Agriculture and Rural Affairs/Institute of Agricultural Resources and Regional Planning, Chinese Academy of Agricultural Sciences, Beijing 100081, China; xubin@caas.cn

* Correspondence: yangxiuchun@bjfu.edu.cn

Abstract: The increasing frequency of global drought events poses a significant threat to the stability of grassland ecosystems' functionality. The Inner Mongolian grasslands stand out as one of the world's most drought-prone regions, facing elevated drought risks compared to other biomes. An in-depth comprehension of the impact of drought on grassland ecosystems is paramount for their long-term sustainability. Using the Standardized Precipitation Evapotranspiration Index (SPEI) from 1982 to 2018, this study identified various drought events within the Inner Mongolian grasslands, encompassing moderate drought, severe drought, and extreme drought. The resistance of the vegetation to the different drought conditions, assessed through net primary productivity (NPP) as a metric (reflecting its capacity to maintain its original level during drought periods), was examined. The research findings indicated that the period from 2001 to 2018 witnessed a substantial increase in both the frequency and the extent of drought events compared to the period from 1982 to 2000, particularly concerning severe and extreme droughts. The areas most severely impacted by extreme drought were the Xilingol League and the Alxa League. From 1982–2000 to 2001–2018, under moderate drought conditions, vegetation resistance exhibited a minor decrease in the central and eastern regions but experienced a slight increase in the western region. In contrast, under severe drought conditions, the western region saw a significant decrease in vegetation resistance. Remarkably, under extreme drought conditions, the western region showed a substantial increase in vegetation resistance, while the central and eastern regions experienced a slight decrease. Across all three drought conditions, as precipitation levels declined, the resistance of the meadow–steppe–desert ecosystems demonstrated a high–low–high distribution pattern. The temperate desert steppe exhibited a minimal vulnerability to drought, boasting resistance levels exceeding 0.9. Notably, extreme drought had the most pronounced impact on the temperate meadow steppe, temperate steppe, and temperate desert steppe, particularly within the temperate meadow steppe category. Given these findings, the authorities responsible for grassland management should prioritize regions characterized by frequent drought occurrences and low drought resistance, such as Ulanqab City, the Xilingol League, and the western part of Hulun Buir City. Safeguarding steppe ecosystems is of paramount importance for stabilizing vegetation productivity and land carbon sinks, especially under the anticipated exacerbation of climate conditions in the future.

Keywords: drought; resistance; grassland; Inner Mongolia; standardized precipitation evapotranspiration index; net primary production



Citation: Guo, J.; Yang, X.; Jiang, W.; Xing, X.; Zhang, M.; Chen, A.; Yang, D.; Yang, M.; Wei, L.; Xu, B.

Resistance of Grassland under Different Drought Types in the Inner Mongolia Autonomous Region of China. *Remote Sens.* **2023**, *15*, 5045. <https://doi.org/10.3390/rs15205045>

Academic Editor: Gabriel Senay

Received: 8 September 2023

Revised: 7 October 2023

Accepted: 18 October 2023

Published: 20 October 2023



Copyright: © 2023 by the authors. Licensee MDPI, Basel, Switzerland. This article is an open access article distributed under the terms and conditions of the Creative Commons Attribution (CC BY) license (<https://creativecommons.org/licenses/by/4.0/>).

1. Introduction

Climate, as an important research field in global change, is directly related to the sustainable development of society, economy, and ecology [1]. In the context of climate change, drought has become one of the most severe natural disasters in the world, causing significant losses to ecosystems and human society [2,3]. Studying how vegetation responds to drought events is a challenging task [4]. Drought can have an impact on the functioning and stability of terrestrial ecosystems [5], especially grassland ecosystems [6]. Future climate change will increase the frequency and intensity of drought in most regions globally, particularly in semi-arid areas under high water resource stress [7,8]. The stability of meadow grassland and steppe grassland ecosystems is susceptible to changes in drought frequency and severity [9,10]. Therefore, it is of great significance to improve our understanding of historical drought dynamics and their impact on grassland ecosystems, especially in the Inner Mongolian grasslands, which are considered one of the ecosystems most vulnerable to water resource stress [11].

The Inner Mongolian grasslands are one of the driest regions in the world, and droughts frequently occur in this grassland ecosystem [12]. Currently, precipitation control experiments have been used to simulate extreme droughts, and a substantial amount of research has been conducted on the resistance of grasslands [13–15]. Previous studies analyzed the impact of different drought types on Net Primary Productivity (NPP) using data from six different grassland sites and meteorological stations through the Standardized Precipitation Index (SPI) analysis [16]. Although the effects of different drought levels on vegetation resistance have been observed at the site scale, it is still necessary to assess the characteristics of resistance under different droughts occurring over a long period at the regional pixel scale. This assessment is of great value for understanding the impact of future drought events of the same magnitude on vegetation. The characteristics of drought events simulated in controlled experiments differ from those occurring naturally, making it important to use existing drought indices to identify historical drought events and evaluate their impact on grassland resistance [17,18]. Ecosystem stability refers to the ability of an ecosystem to maintain balance and functional integrity, such as the ability to sustain production under drought conditions, which is known as ecosystem resistance [19].

The advantages of remote sensing technology in long time-series and large scale can be used to assess the resistance of vegetation under historical drought states [20]. NPP has often been used to evaluate plant growth, and insufficient precipitation has a great impact on NPP in grasslands. Therefore, NPP can be used as a suitable index to evaluate the impact of drought on grasslands' productivity [16], and it is necessary for analyzing the impact of different drought levels, at the regional scale, in long time-series, on the resistance of different grassland types. Many drought indices have been used to represent climatic conditions, such as the Standardized Precipitation Evapotranspiration Index (SPEI), the SPI, the Standardized Terrestrial Water Storage Index (STI), and the Palmer Drought Severity Index (PDSI) [17,21–23]. The SPEI is a simple and physically relevant drought index calculated based on the difference between potential evapotranspiration and precipitation, which is better than the drought index calculated using only temperature and precipitation for reflecting the water stress of ecosystems [24]. Therefore, the SPEI values of different time-scales can be used to quantify large-scale and long-term drought, especially in semi-arid and arid regions [25,26].

Grassland accounts for about 40% of China's total land area [27]. The grassland coverage in Inner Mongolia accounts for 55.4% of the total area [28] and 20% of China's total grassland area [29]. Grasslands play an extremely important economic role for the population from this region. Gaining a deeper understanding of the functions of and threats to grasslands is of great significance for the sustainable development of grasslands and for coping with climate change. The latest research shows that the Inner Mongolia Autonomous Region was the area in China most affected by drought during 1991–2018, considering factors including the affected area, livestock numbers, crop yields, economy, etc. [30].

In this study, we used the NPP and SPEI data to assess the ecological stability of different grassland types in Inner Mongolia, China, during 1982–2018. Therefore, the purposes of this study are the following: (1) to assess the spatiotemporal distribution characteristics of different drought types (moderate drought, severe drought, and extreme drought) during 1982–2018; (2) to investigate the spatial distribution characteristics of resistance under different drought types; and (3) to examine the resistance characteristics of different grassland types under different types of droughts.

2. Materials and Methods

2.1. Study Area

Located in northern China, the Inner Mongolia grasslands ($97^{\circ}12'E\sim 126^{\circ}04'E$, $37^{\circ}24'N\sim 53^{\circ}23'N$) have a high biodiversity and important ecological functions (Figure 1). They are part of the Eurasian grasslands and a major production base of animal husbandry resources in China. From west to east, there are mainly three types of grassland ecosystems: desert, steppe, and meadow. There are seven main grassland types, and the average annual precipitation is as follows, from low to high: temperate desert (TD, 180 mm), temperate steppe desert (TSD, 193 mm), temperate desert steppe (TDS, 210 mm), temperate steppe (TS, 299 mm), lowland meadow (LM, 357 mm), temperate meadow steppe (TMS, 383 mm), and upland meadow (UM, 404 mm). However, in recent years, climate change and the intensification of human activities have led to the deterioration of ecological environments, grasslands' degradation and desertification, and the occurrence of grassland droughts, which have seriously affected grass-based husbandry [31]. In order to reduce the change in grassland type caused by climate fluctuation and human activities, the unchanged grasslands from 1980 to 2020 were selected for research. The land use/land cover data with a spatial resolution of 1 km were obtained from the Resource and Environment Science and Data Center, of the Institute of Geographic Sciences and Natural Resources Research, at the Chinese Academy of Science.

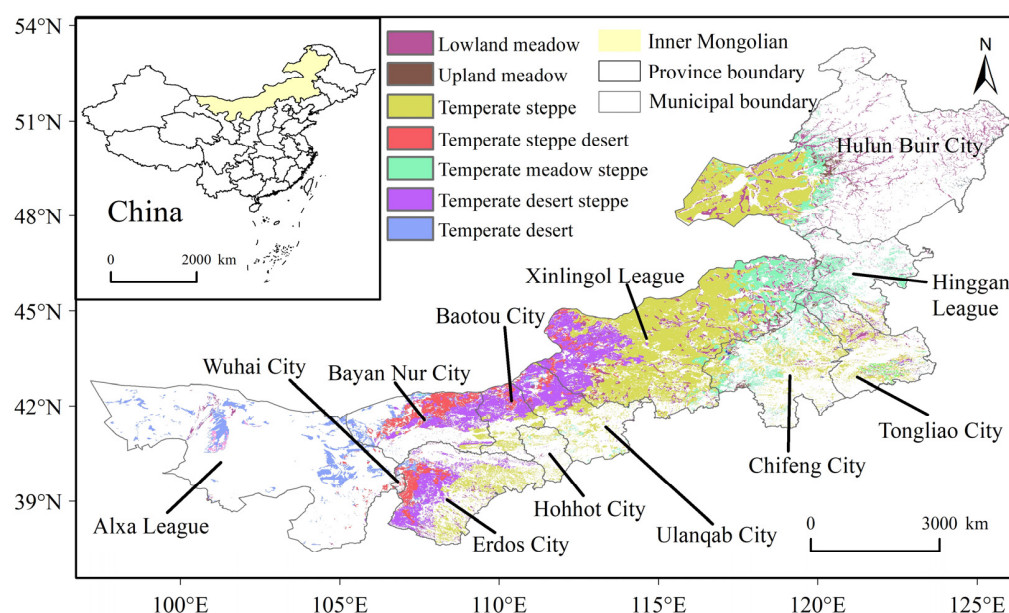


Figure 1. Geographical maps of Inner Mongolia showing various administrative divisions and the distribution of different grassland types.

2.2. SPEI Data

SPEI is calculated by estimating the “climate water balance”, which measures the deviation between precipitation and potential evapotranspiration. The SPEI is then adjusted to a probability distribution to convert the origin values to comparable normalized units in

space and time [32]. To identify extreme drought events, the SPEI data [4,23,33] were obtained from the global SPEI dataset, which was provided by the Climatic Research Unit of the University of East Anglia (<http://sac.csic.es/spei/database.html> accessed on 18 April 2022). The SPEI was calculated based on monthly precipitation and potential evapotranspiration. This data provided SPEI timescales between 1 and 48 months, with a half-degree spatial resolution and a monthly temporal resolution. The growing season of grassland vegetation in Inner Mongolia extends from April to September, which is also the period with the highest proportion of precipitation throughout the year. We used a 6-month time-scale SPEI-06 of September to determine the drought type, because the SPEI-06 of September was calculated based on the data from April to September, which could best investigate growing-season drought. The SPEI data of April–September over 30 years (1982–2018) were chosen for the analysis. Based on its SPEI value, the climate of each year was classified into four categories (Table 1): extreme drought ($\text{SPEI} \leq -2$), severe drought ($-2 < \text{SPEI} \leq -1.5$), moderate drought ($-1.5 < \text{SPEI} \leq -1$), and near normal ($-1 < \text{SPEI} \leq 1$) [26,34,35].

Table 1. List of climate categories.

Category	SPEI
Extreme drought	$\text{SPEI} \leq -2$
Severe drought	$-2 < \text{SPEI} \leq -1.5$
Moderate drought	$-1.5 < \text{SPEI} \leq -1$
Near normal	$-1 < \text{SPEI} \leq 1$

2.3. NPP Data

NPP was selected as an indicator of grassland vegetation growth conditions. The annual NPP remote sensing data were derived from the Global Land Surface Satellite (GLASS) product suite (<http://www.glass.umd.edu/> accessed on 18 April 2022) at a spatial resolution of 0.05 degrees. The annual NPP data of 1982–2018 were downloaded and resampled at a spatial resolution of 1 km using ArcGIS.

2.4. Calculation Method of Grassland Drought Resistance

Resistance is defined as the ability of an ecosystem to maintain production under drought conditions [19]. The ratio of the NPP during extreme drought periods to the NPP during multiple years of normal growth ($-1 < \text{SPEI} \leq 1$) was calculated using the following equation to control the confounding effect of the conditions in the previous year:

$$\text{RES} = \frac{\text{NPP}_{\text{drought}}}{\text{NPP}_{\text{normal}}}$$

where RES represents the resistance under drought; $\text{NPP}_{\text{drought}}$ represents the NPP in the drought year; and $\text{NPP}_{\text{normal}}$ represents the average NPP during multiple years of normal growth (1982–2018) ($-1 < \text{SPEI} \leq 1$).

2.5. Research Framework

The research framework of the key indicators' computation and statistical analysis is displayed in Figure 2.

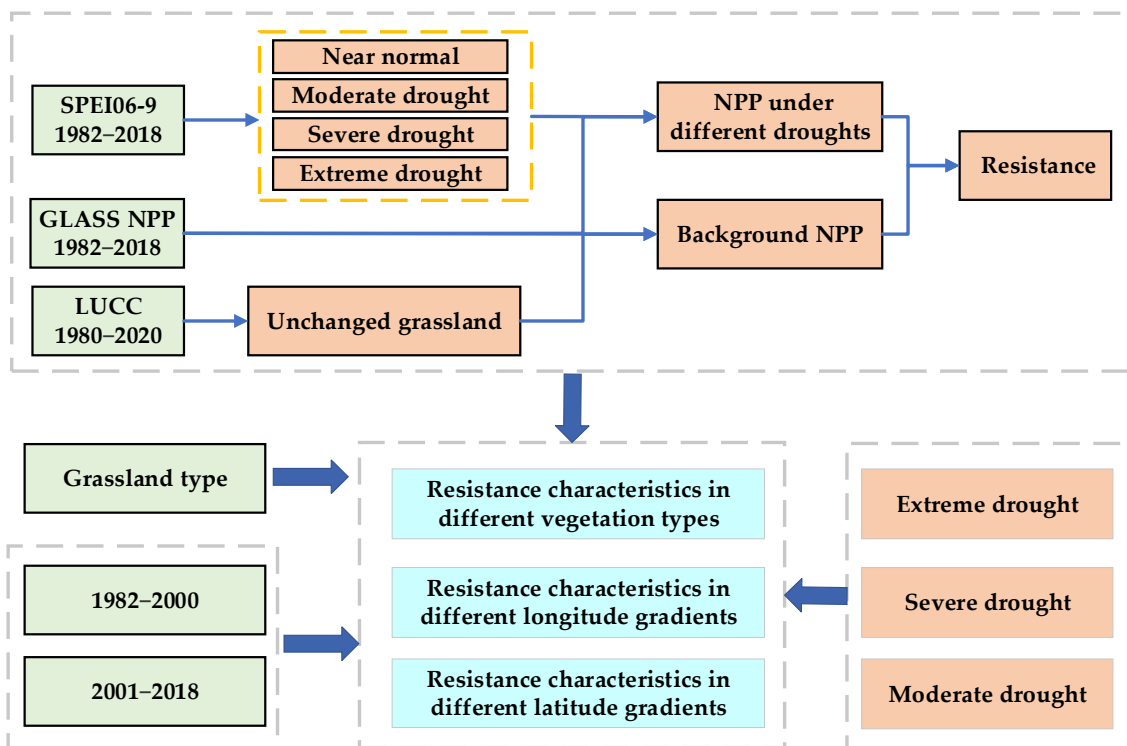


Figure 2. Research framework used in this study.

3. Results

3.1. Spatiotemporal Characteristics of Different Droughts from 1982 to 2018

Figure 3 illustrated the spatial distribution of moderate drought, severe drought, and extreme drought frequency during 1982–2000. During 1982–2000, the regions affected by moderate drought, severe drought, and extreme drought accounted for 94.68%, 58.22%, and 23.45%, respectively. During 1982–2000, moderate drought was observed in 91.83% of the regions, occurring one–four times. Areas experiencing more than four instances of moderate drought were primarily concentrated in the eastern part of the Xilin Gol League, in Bayan Nur City, in the Alxa League, and in Erdos City. Severe drought occurrences were mainly limited to one or two instances during the years from 1982 to 2000, with areas lacking severe drought being mainly distributed in the eastern region. Extreme drought, during the 1982–2000 period, was observed in only 23.45% of the areas, primarily occurring once or twice. These extreme drought events were concentrated in Chifeng City and Tongliao City in the southeast, as well as in Bayan Nur City and Erdos City in the west.

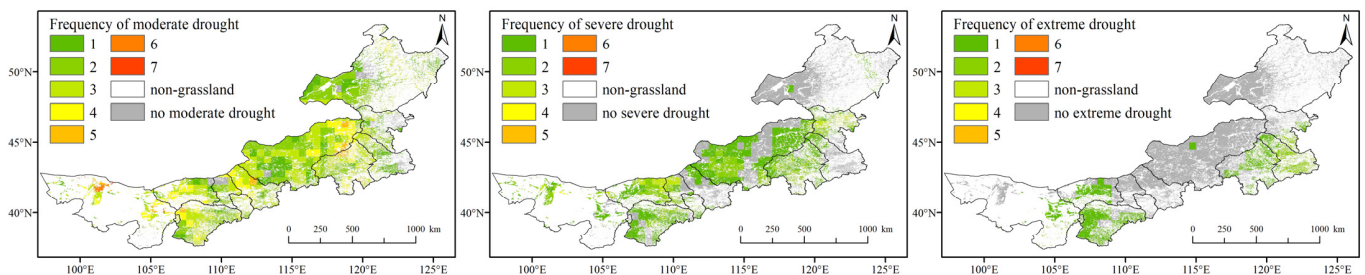


Figure 3. Spatial distribution of the frequency of moderate drought, severe drought, and extreme drought during 1982–2000.

Figure 4 illustrates the spatial distribution of the frequency of moderate drought, severe drought, and extreme drought during 2001–2018. During 2001–2018, there was a

gradual expansion in both the extent and frequency of drought. During this timeframe, the proportion of areas experiencing moderate drought one–five times was 93.06%. Notably, the frequency of one–three times decreased, while the frequency of four–five times increased. The areas with a frequency of four–five times were primarily concentrated in the Xilin Gol League, in the central and southwestern regions of Hulun Buir City, in Bayan Nur City, and in the western Alxa League. There was a significant increase in the frequency of areas experiencing severe drought two–five times, accompanied by a notable expansion in the extent of severe drought. The areas with a frequency of four–five times were predominantly found in the southwest of the Xilin Gol League and in Ulanqab City. In stark contrast, 97.29% of the areas experienced extreme drought during 2001–2018, with the frequency of areas mainly experiencing extreme drought two–four times reaching 85.55%, significantly higher than that observed during 1982–2000. The areas with a frequency of four and five extreme drought events were primarily situated in the Xilin Gol League and in the Alxa League.

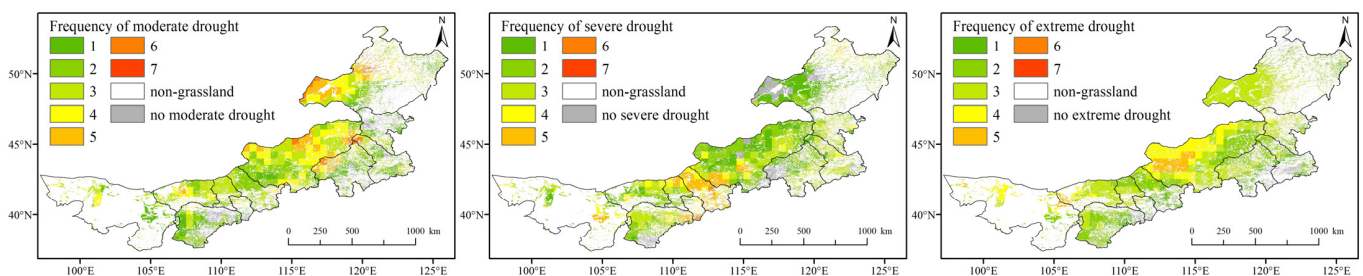


Figure 4. Spatial distribution of the frequency of moderate drought, severe drought, and extreme drought during 2001–2018.

Figure 5 shows the annual proportion of areas affected by moderate drought, severe drought, and extreme drought. Before the year 2000, the proportion of areas experiencing moderate drought, severe drought, and extreme drought was relatively small. Extreme drought events were recorded in 1982 (4.53%), 1991 (12.09%), and 1999 (1.29%). In the years with severe drought affecting over 5% of the total area, notable occurrences took place in 1982 (8.71%), 1989 (10.40%), 1991 (7.77%), and 1999 (12.81%). There were 11 years with an area proportion of severe drought measuring less than 1%. The extent of moderate drought began to increase gradually from 1989 onwards, with proportions exceeding 25% in 1989 (25.03%), 1997 (47.66%), and 1999 (54.3%). Before the year 2000, areas experiencing moderate drought below 10–20% were noted in 1982 (12.29%), 1986 (13.94%), and 1995 (12.43%). Since 2000, there has been a significant expansion in the scope of drought. The average annual area affected by drought increased from 14.54% to 45.59%, marking a more than threefold increase. Specifically, the average annual area affected by moderate drought increased from 10.85% to 16.86%; the average area affected by severe drought increased from 2.69% to 13.55%, and the average area impacted by extreme drought rose from 1.00% to 15.18%. The increases in severe drought and extreme drought were particularly significant. Severe drought affected more than 20% of the total area in 2000 (33.29%), 2001 (22.29%), 2005 (21.69%), 2009 (33.17%), 2015 (25.92%), and 2017 (32.90%). The area affected by extreme drought after 2000 exhibited an initial increase, followed by a sharp decrease, reaching its peak in 2010, when more than two-thirds of the total area were impacted.

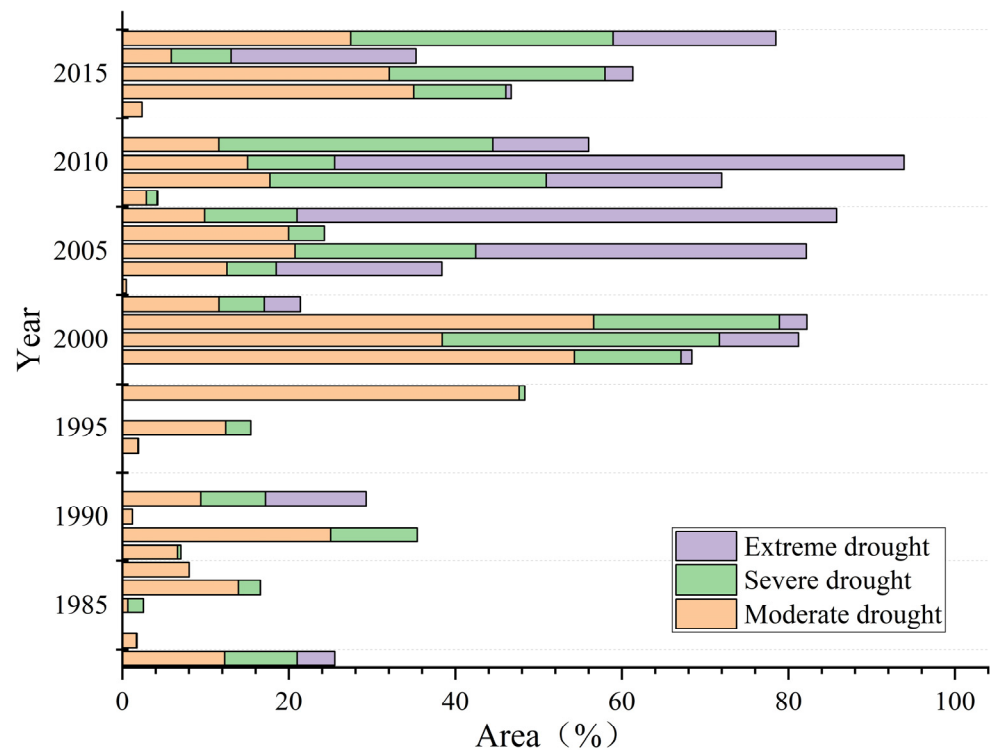


Figure 5. Annual area proportion of moderate drought, severe drought, and extreme drought during 1982–2018 (%).

3.2. Spatial Distribution Characteristics of Resistance under Different Drought Types

3.2.1. Resistance under Moderate Drought

The temporal and spatial distribution of resistance under moderate drought from 1982 to 2000 (Figure 6(a1)) revealed lower resistance levels in the central part, primarily concentrated in the western Xilingol League, while resistance was higher in eastern and western Inner Mongolia. Figure 6(a2) shows the resistance changes with the latitude. It became evident that high-latitude regions exhibited greater resistance, with all the areas north of 45.2°N having resistance values exceeding 0.9, indicating a lesser impact from moderate drought. The resistance gradually decreased from 45.2°N to 42°N , then demonstrated an increasing–decreasing–increasing trend from 42°N to 38.5°N . South of 38.5°N , the resistance dropped from 0.91 to 0.53. Figure 6(a3) shows the resistance changes with the longitude. The resistance in the western regions of the moderately arid grasslands fluctuated significantly from 1982 to 2000, primarily in the Alxa League, while the eastern regions exhibited smaller fluctuations. Declining trends were noticeable between 103°E – 108.5°E and 110°E – 113°E , whereas an increasing trend was mainly observed between 113°E and 126°E , with resistance values exceeding 0.9 beyond 116°E , indicating minimal impact from moderate drought.

Figure 6(b1) shows the temporal and spatial distribution of the resistance to moderate drought from 2001 to 2018. It was similar to the resistance distribution from 1982 to 2000, but the resistance decreased in the central and eastern regions while increasing in the western regions. Resistance changing with the latitude (Figure 6(b2)) revealed a noticeable decrease in the resistance in high-latitude regions and a significant increase in low-latitude areas. The areas south of 41.8°N generally had resistance values above 0.9, and the areas north of 49.9°N mostly exhibited resistance values greater than 0.9, with both regions experiencing minimal vegetation impact from moderate drought. Between 49.9°N and 48.5°N , there was a decreasing trend, and, between 48.5°N and 42.8°N , the resistance fluctuated between 0.8 and 0.9, with the lowest values occurring between 42.1°N and 42.7°N , where the resistance ranged from 0.7 to 0.8. Figure 6(b3) shows the resistance changes with the longitude. The

fluctuation pattern of the resistance to the moderate drought from 2001 to 2018 mirrors that of 1982–2000. The numerical values of the resistance in the central and eastern regions were lower compared to 1982–2000. East of 110°E , the resistance sharply decreased, with the lowest values occurring between 111°E and 113.4°E , ranging from 0.65 to 0.7. The areas east of 118°E had resistance values above 0.9, indicating minimal impact from moderate drought.

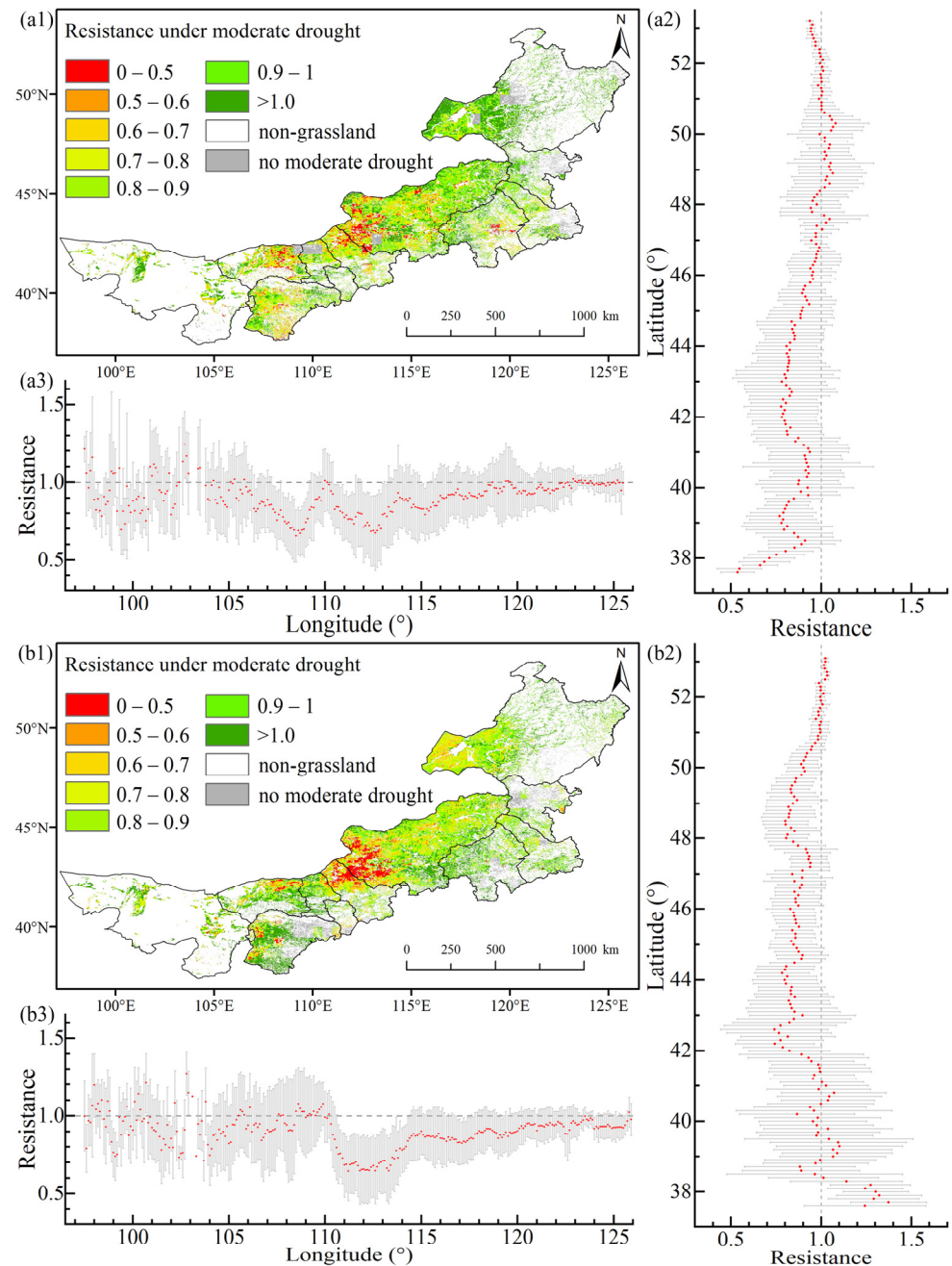


Figure 6. Spatial distribution of grassland resistance under moderate drought in Inner Mongolia during 1982–2000 and 2001–2018. (a1–a3) show spatial distribution of resistance, resistance characteristics in different longitude gradients, and resistance characteristics in different longitude gradients during 2001–2018, respectively. (b1–b3) show spatial distribution of resistance, resistance characteristics in different longitude gradients, and resistance characteristics in different longitude gradients during 1982–2000, respectively. The red dots and grey lines in (a2,a3,b2,b3) show average resistance at latitude/longitude and error bar (± 1 standard error).

3.2.2. Resistance under Severe Drought

The spatial distribution of resistance during 1982–2000 under severe drought (Figure 7(a1)) revealed areas with lower resistance situated in the northwestern part of the Xilingol League and in the southwestern part of Hulun Buir City. Resistance changing with the latitude (Figure 7(a2)) indicated that high-latitude regions exhibited a higher resistance, with all the areas north of 50.5°N having resistance values greater than 0.9, indicating a lesser impact from severe drought. The resistance decreased from 0.94 to 0.67 from 50.5°N to 49.5°N , while the resistance mostly fluctuated between 0.7 and 0.9 from 42.2°N to 49.5°N . From 42.2°N to 38°N , the resistance gradually rose from 0.75 to 1.2, but, south of 38°N , the resistance fluctuated dramatically, showing a decline. Figure 7(a3) shows the resistance changes with the longitude. It is evident that the resistance under severe drought fluctuated significantly west of 110.4°E , with a resistance mostly above 0.9. Between 110.5°E and 120°E , the grassland resistance ranged from 0.7 to 0.85, and, east of 120°E , the resistance increased, particularly east of 123°E , where the resistance could reach above 0.95.

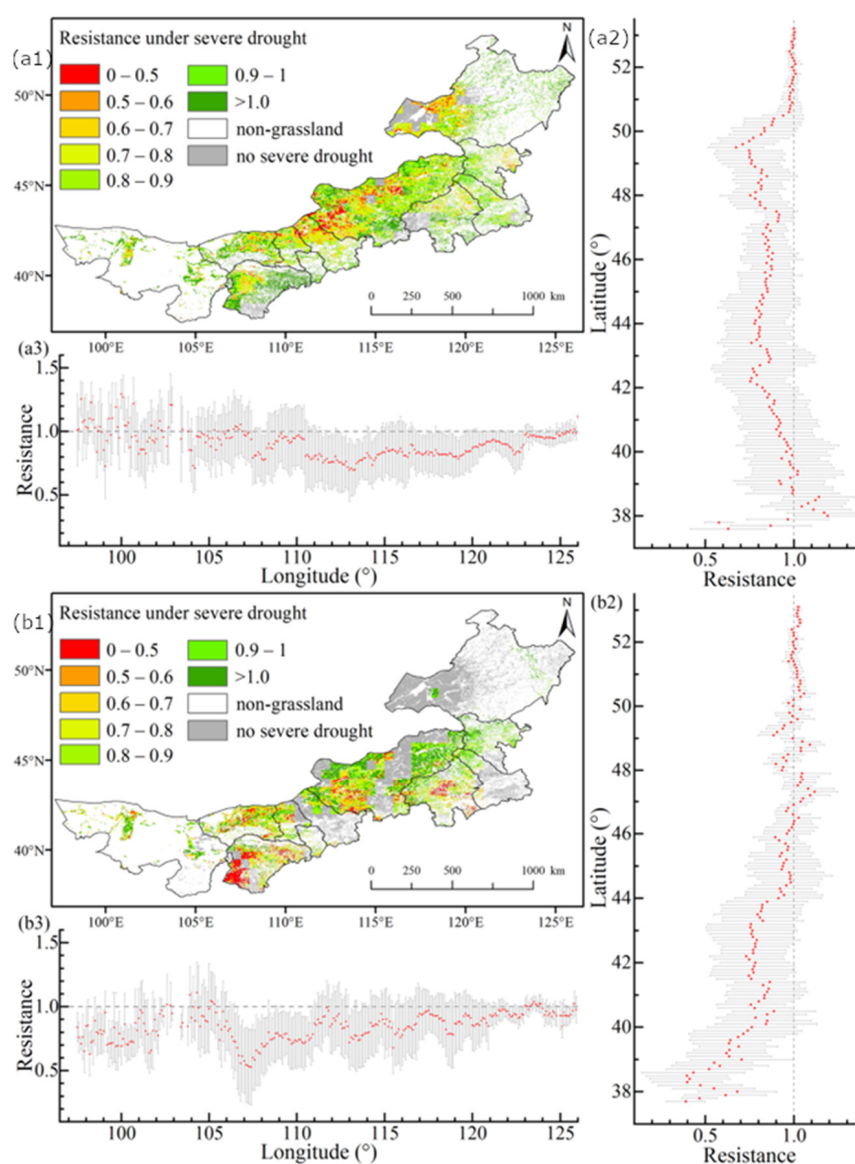


Figure 7. Spatial distribution of grassland resistance under severe drought in Inner Mongolia during 1982–2000 and 2001–2018. (a1–a3) show spatial distribution of resistance, resistance characteristics in

different longitude gradients, and resistance characteristics in different longitude gradients during 1982–2000, respectively. (b1–b3) show spatial distribution of resistance, resistance characteristics in different longitude gradients, and resistance characteristics in different longitude gradients during 2001–2018, respectively. The red dots and grey lines in (a2,a3,b2,b3) show average resistance at latitude/longitude and error bar (± 1 standard error).

Figure 7(b1) shows the spatial distribution of the resistance under severe drought during 2001–2018. It is evident that Ordos City and Chifeng City exhibited a significant decrease in resistance compared to 1982–2000, while central regions showed a slight increase in resistance. Resistance changing with the latitude (Figure 7(b2)) indicated that the areas north of 44°N exhibited a noticeable increase in resistance compared to 1982–2000, with resistance values mostly above 0.9. The areas south of 44°N showed a significant decrease in resistance compared to 1982–2000, with resistance mostly ranging from 0.75 to 0.85 between 43.7°N and 40°N , and a decrease from 0.74 to 0.58 between 40°N and 38.8°N . Figure 7(b3) shows the resistance changes with the longitude. It was observed that most of the areas below 103°E and between 105°E and 110.7°E exhibited a significant decrease in resistance compared to 1982–2000, while the areas above 110.7°E showed varying degrees of increase in resistance compared to 1982–2000. The regions above 119.4°E could have resistance values above 0.9, indicating minimal impact from severe drought.

3.2.3. Resistance under Extreme Drought

The spatial distribution of the resistance under extreme drought during 1982–2000 (Figure 8(a1)) revealed that the areas experiencing extreme drought were relatively small. The regions with the lowest resistance were located in the western parts of the Bayannur and Erdos cities, while Chifeng City exhibited a higher resistance. Figure 8(a2) shows the resistance changing with the latitude under extreme drought. It is evident that low-latitude areas (less than 39.1°N) generally had resistance values below 0.7. The region between 39.2°N and 46.4°N showed a resistance mostly fluctuating between 0.7 and 0.9. Figure 8(a3) shows the resistance changing with the longitude under extreme drought. There was a decreasing trend in resistance between 101°E and 109.4°E , where the resistance decreased from 1.23 to 0.59. Between 114.4°E and 123.3°E , there was a gradual decrease in resistance, with values dropping from 1.11 to 0.75.

The spatial distribution of the resistance under extreme drought during 2001–2018 (Figure 8(b1)) revealed that the resistance was higher in the western and eastern regions, while most of the areas in the central region exhibited a lower resistance. Figure 8(b2) shows the resistance changing with the latitude. The low-latitude areas showed a significant increase in resistance compared to 1982–2000, with resistance values exceeding 0.7. There was a decreasing trend between 37.6°N and 38.7°N , while an increasing trend was observed between 38.7°N and 39.5°N . The region from 39.5°N to 46°N exhibited a gradual decline in resistance, with values decreasing from 1.05 to 0.68. The resistance in the 46°N to 48°N range initially increased and then decreased, stabilizing between 48.1°N and 49.6°N at 0.7–0.75. Beyond 49.7°N , the resistance gradually increased to 0.97. The high-latitude regions were less affected by extreme drought. Figure 8(b3) shows the resistance changing with the longitude under extreme drought. The areas below 107°E experienced relatively significant fluctuations in resistance, with the resistance ranging between 0.8 and 1.2. Between 107°E and 111°E , the resistance initially increased to 1.04 and then decreased to 0.7. The region between 111°E and 119.4°E showed a minimal variation in the resistance, fluctuating between 0.7 and 0.8. Beyond 119.4°E , the resistance exhibited a gradual increase over time.

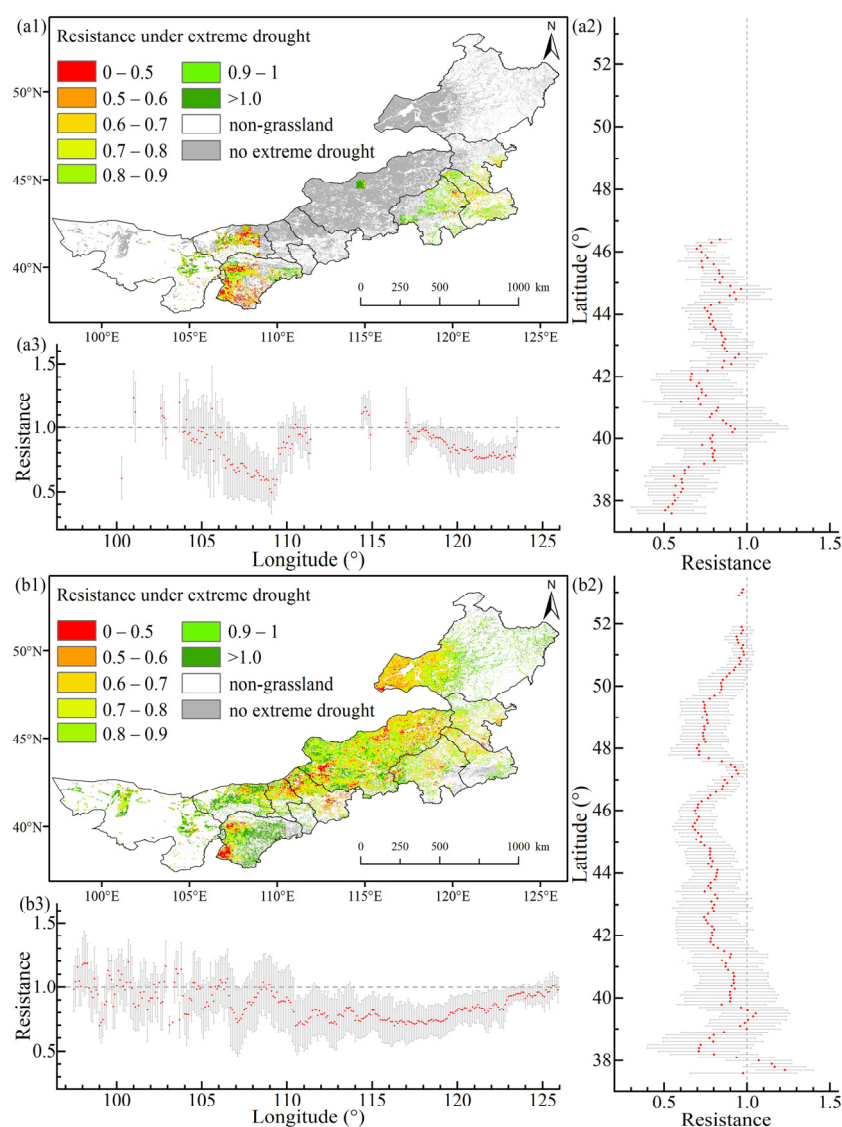


Figure 8. Spatial distribution of grassland resistance under extreme drought in Inner Mongolia during 1982–2000 and 2001–2018. (a1–a3) show spatial distribution of resistance, resistance characteristics in different longitude gradients, and resistance characteristics in different longitude gradients during 1982–2000, respectively. (b1–b3) show spatial distribution of resistance, resistance characteristics in different longitude gradients, and resistance characteristics in different longitude gradients during 2001–2018, respectively. The red dots and grey lines in (a2,a3,b2,b3) show average resistance at latitude/longitude and error bar (± 1 standard error).

3.3. Resistance Characteristics in Different Grassland Types under Different Droughts

Figure 9 depicts the resistance characteristics of seven grassland types to different drought intensities during 1982–2000. The grassland types are arranged from left to right, with an average annual precipitation gradually decreasing from 404 mm to 180 mm. It was observed that, as the annual precipitation decreased, the resistance of these grassland types decreased, from being at its highest in the UM to being at its lowest in the TDS, with a gradual increase in the TD. Among the types, the TDS (0.76, resistance) and the TSD (0.78) were significantly affected by moderate drought, with four types (UM, TMS, LM, and TD) showing resistance values above 0.9, thus indicating a high capacity to withstand moderate drought. Under severe drought, the TD exhibited the highest resistance at 0.93, while the TDS had the lowest resistance at 0.78, with the other types showing resistance values between 0.8 and 0.9. Even under extreme drought, the TD maintained a resistance

above 0.9, while the TDS and TSD exhibited a lower resistance, dropping below 0.7. The TD consistently maintained a resistance above 0.9 across all three drought types, showing minimal sensitivity to drought. The LM, TS, TDS, and TSD exhibited the lowest resistance under extreme drought conditions. The TDS and TSD displayed a higher resistance under severe drought conditions compared to moderate and extreme drought. The LM and TS experienced a decreased resistance as drought severity increased. The UM, TMS, and TD, on the other hand, maintained resistance levels under extreme drought conditions even slightly higher than those under severe drought conditions. Looking at the standard deviation of the resistance fluctuation for each type, it was observed that, as the annual precipitation decreased, the fluctuation in resistance gradually decreased.

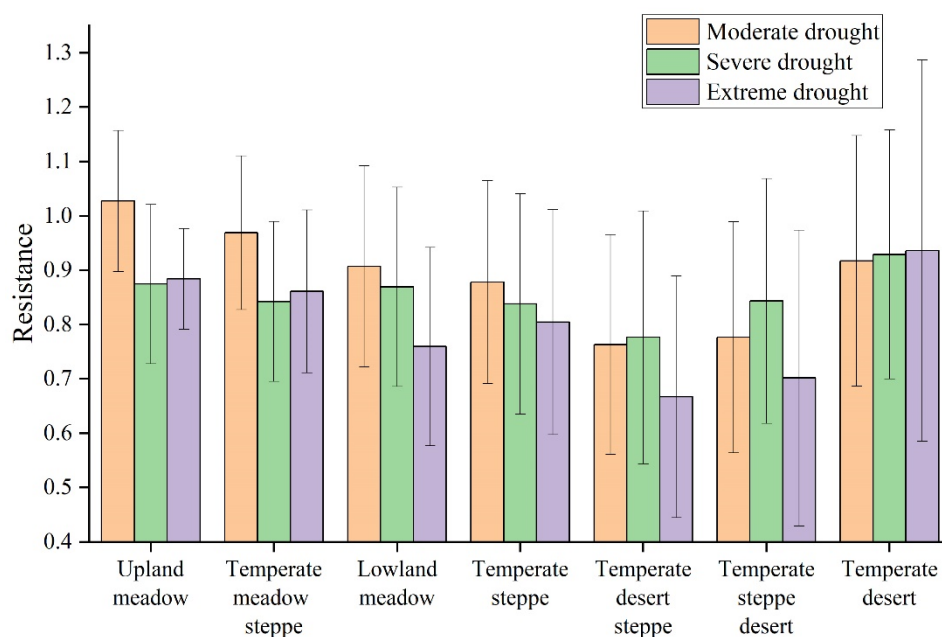


Figure 9. Average resistance of seven grassland types under different drought types during 1982–2000.

Figure 10 depicts the resistance characteristics of seven grassland types to different drought intensities during the period from 2001 to 2018. Across the three drought types, arranged in a gradient of decreasing precipitation from high to low, the trend in resistance change was consistent with that observed from 1982 to 2000, characterized by an initial decrease, followed by an increase. The TDS (0.78) was notably affected by moderate drought, while types with a resistance exceeding 0.9 included the highest precipitation-dependent UM and the lowest precipitation-dependent TD. Under severe drought conditions, the TDS (0.75) and TSD (0.73) exhibited a significant impact, with the UM and TMS showing a resistance above 0.9. Additionally, the UM and TMS exhibited a higher resistance compared to the moderate and extreme drought. Extreme drought significantly affected the UM and TMS, causing a noticeable decline in resistance. The LM and TS showed a slight decrease in resistance under severe drought conditions. However, the two desert types that tended towards arid conditions, namely, the TSD (0.86) and the TD (0.95), displayed the highest resistance under extreme drought. The meadow-type resistance ranged from 0.83 to 0.86, while the three steppe types exhibited the lowest resistance, ranging from 0.75 to 0.8. In terms of resistance fluctuation, similarly to the period from 1982 to 2000, as the annual precipitation decreased, the resistance fluctuation increased, as indicated by a higher standard deviation.

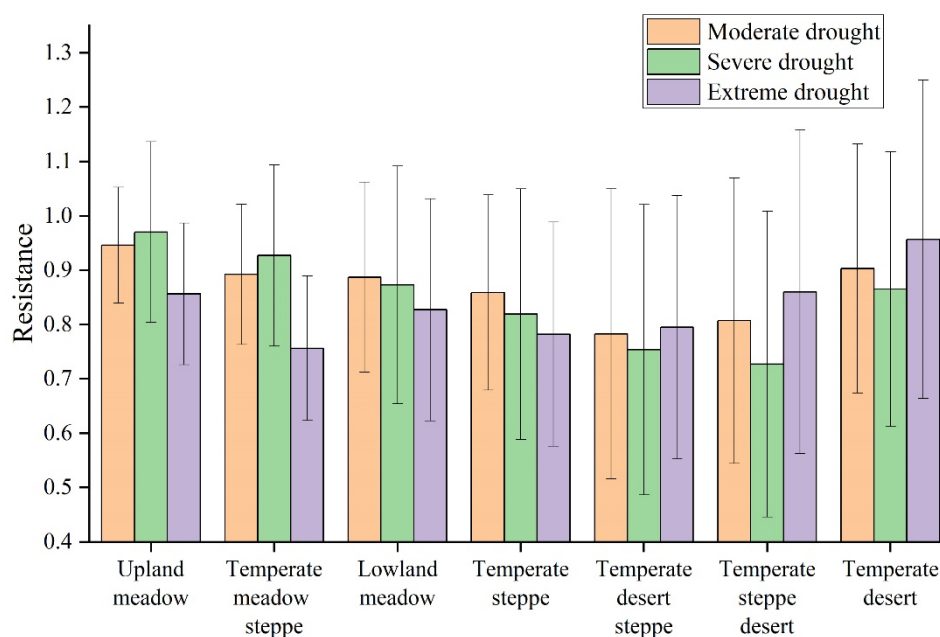


Figure 10. Average resistance of seven grassland types under different drought types during 2001–2018.

4. Discussion

4.1. Characteristics of Drought Occurrence

The IPCC report had indicated a significant increase in the extent and intensity of global-scale droughts in recent decades, with a particular rise in extreme drought events [36]. In our study, we used the 1982–2018 SPEI dataset to extract annual occurrences of moderate, severe, and extreme drought events. The study period was divided into two intervals, 1982–2000 and 2001–2018. The results revealed that, during the second period, both the range and frequency of all the drought types were greater than those in the first period. Particularly striking was the increase in the occurrence range of extreme drought, soaring from 23.45% to 97.29%, along with a rise in frequency, from one–two events to two–four events. This finding was in alignment with the conclusions drawn in the IPCC report.

Previous research had also indicated the intensification of drought in Inner Mongolia, with this trend beginning around 1997 [37]. Our results further corroborated this trend by revealing that the drought area exceeded 40% in 1997, whereas it had been below 40% before 1997, thereby highlighting 1997 as a pivotal year for drought. Another study focusing on Inner Mongolia’s drought from 1982 to 2013 had highlighted a prolonged period of drought from 1999 to 2011 [38]. Our segmentation analysis with the mid-point year 2000 closely aligned with this timeframe.

The regions with the highest frequency of all three drought types were predominantly concentrated in the central and western regions, mainly characterized by desert and steppe landscapes. These areas, being arid and semi-arid in nature, were inherently susceptible to all three drought types, which is consistent with the findings of previous drought research in Inner Mongolia [31]. Research conducted in Tongliao City, in Inner Mongolia, had suggested a periodic intensification of drought in semi-arid sandy areas from 2007 to 2021, which is in line with our findings [38]. Another study had identified regions with high drought intensity in Inner Mongolia, especially during spring and summer, primarily located in the western and central-western areas [37]. Our drought research primarily focused on the growing season SPEI, covering spring and summer, aligning well with the results of previous research. Furthermore, the study suggested that the significant increase in temperature since 1990 in Inner Mongolia may be one of the reasons for the expansion of drought in terms of both extent and intensity [37].

4.2. Characteristics of Resistance in Different Grassland Types

The ability of different plant species to respond to varying levels of drought varied [39]. As drought intensified, there was a general trend of decreasing resistance for five types of meadow and steppe, except for the desert. Extreme drought significantly impacted plant growth, with the exception of TD, which was consistent with previous research conducted from 1982 to 2012 [40]. The TD, as one of the regions with the least precipitation in the study area and a high frequency of drought occurrence, generally maintained a resistance level above 0.9 under the influence of all drought types in both time periods (except for 0.87 under severe drought in 2001–2018). This could be attributed to the high probability of drought in this region, where vegetation primarily consisted of drought-resistant plant species and the vegetation had adapted to drought conditions.

Experimental results from Inner Mongolia suggested that the decline in aboveground biomass caused by extreme drought was mainly due to a reduction in non-dominant species. Many weeds had simpler taproots compared to dominant grasses in the Poaceae, which might have contributed to better drought tolerance [41]. The TD and TSD had fewer species, with dominant species having a significant biomass and well-developed root systems, making them more resistant to extreme drought. This was likely one of the reasons for their resilience.

Soil moisture conditions in loamy soils were higher than in sandy soils, resulting in a higher NPP. This higher NPP led to increased litter cover, which, in turn, enhanced the soil's physical properties by increasing the soil's organic matter content. This formed a positive feedback loop. Moreover, a thicker litter layer and higher soil organic carbon effectively prevented soil moisture evaporation and plant transpiration loss. Under drought conditions, higher soil water retention and lower evapotranspiration in loamy soils resulted in soil moisture levels remaining around 20%, similar to the control plots in the sandy soils under equivalent annual precipitation conditions in Hulun Buir [41]. In the eastern region, dominated by meadows and steppe, the meadows exhibited higher coverage and soil moisture levels than the steppe. The results indicated that, under varying drought types, meadows had a higher resistance compared to steppe; this was consistent with previous research findings [41].

4.3. Factors Influencing Resistance under Drought

The response of fraction vegetation coverage and abundance to drought stress indicated that plant species' resistance was species-specific [39]. Previous studies had mostly shown that, under conditions of insufficient water supply, vegetation coverage decreased [42], leading to a decline in NPP, especially in arid and semi-arid regions [43]. Water was a critical resource for plant growth in semi-arid grasslands and a primary limiting factor for plant growth [44,45]. In different grassland type, extreme drought had varying impacts on aboveground NPP [46], which was consistent with the findings of this study. When external conditions lacked water, plants wilted or even died. Many previous research reports had indicated that changes in community coverage and abundance due to drought were closely related to changes in soil moisture [47]. This study assessed vegetation resistance under moderate drought, severe drought, and extreme drought conditions and found that the areas with the highest and lowest precipitation were meadows and deserts, respectively, with significantly higher resistance compared to steppe, which fell between the two. Under drought conditions, soil moisture in the humid grassland ecosystems was higher than in the arid grassland ecosystems, which may have contributed to a higher resistance to drought [46,48]. The higher resistance of the meadow ecosystems in eastern Inner Mongolia may have been closely related to soil moisture. The significantly higher frequency of extreme drought events in the temperate meadow steppe from 2001–2018 compared to 1982–2000 could have been due to the repeated occurrence of extreme drought in these areas, resulting in a decrease in soil moisture, especially when extreme drought events occurred consecutively for two years, potentially leading to a cumulative drought effect and a reduced resistance with the increasing duration of extreme drought [49]. How-

ever, the TD, which received the least annual precipitation, remained unaffected by the intensity of drought and maintained a high resistance. This could have been attributed to the adaptation of plants in the drought-prone grassland ecosystem, where plant resistance to drought may have been higher compared to wetter grassland ecosystems [50].

In this study, the resistance of the TDS, TSD, and TD under the extreme drought conditions from 2001 to 2018 showed some improvement compared to the period from 1982 to 2000. This could also be indicative of a gradual recovery of the vegetation. Following the peak of drought, especially extreme drought, in 2010, there has been a trend of weakening, and, since 2011, China has implemented grassland subsidy policies in Inner Mongolia, with a cumulative investment of 45.5 billion yuan over the past decade. Proper grazing management, grassland protection, and ecological restoration may contribute to better vegetation growth. Over the past two decades, extreme high-precipitation and extreme drought have been on the rise. Coupled with an increased attention to grassland management in the sector, this might enhance the grassland vegetation's ability to withstand extreme climatic risks. This study also has some limitations as it focused on two distinct time periods. Due to the significant climate fluctuations after 2000, it was not possible to explore the details of resistance between years. Further research is needed to address this issue in the future.

5. Conclusions

We investigated the spatial and temporal characteristics of moderate drought, severe drought, and extreme drought in the Inner Mongolian grasslands from 1982 to 2018, as well as the spatial pattern of vegetation resistance during these drought periods. The differences in resistance among different grassland types were also analyzed. The results showed that both the area and intensity of drought have significantly increased since 1997, with the most severe occurrence of extreme drought happening in the Xilingol League and in the Alxa League. Under the three drought types, the resistance of the meadow–grassland–desert showed a high–low–high distribution as precipitation decreased. The warm desert was minimally affected by the three droughts, with resistance reaching above 0.9. Extreme drought had the greatest impact on the temperate meadow steppe, the temperate steppe, and the temperate desert steppe, mainly distributed in Ulanqab City, in the Xilingol League, and in the western part of Hulun Buir City. This leads us to conclude that the semi-arid grassland ecosystem is most susceptible to drought events, especially the temperate meadow steppe and the temperate steppe, and that the resistance in 2001–2018 has decreased compared to 1982–2000. Given the expected increase in severity and duration of future droughts, our research findings may help identify the most vulnerable vegetation areas in Inner Mongolia, enabling relevant measures to be taken by government departments to address climate change.

Author Contributions: Conceptualization, J.G. and X.Y.; software, J.G. and M.Z.; formal analysis, J.G., A.C. and M.Y.; data curation, J.G., X.X., D.Y. and L.W.; writing—original draft preparation, J.G.; writing—review and editing, J.G., X.Y., W.J. and B.X.; funding acquisition, X.Y. All authors have read and agreed to the published version of the manuscript.

Funding: This work was supported by the Third Comprehensive Scientific Expedition in Xinjiang [2022xjkk0402].

Data Availability Statement: The data presented in this study are available on request from the corresponding author.

Acknowledgments: We would like to thank the editor and anonymous reviewers for their valuable comments and suggestions for this paper. We are also grateful to the Data Center for Resources and Environmental Sciences, at the Chinese Academy of Sciences (RESDC) (<http://www.resdc.cn>, accessed on 7 September 2023). We thank the editor and anonymous reviewers of the journal for their valuable comments and suggestions that helped improve this paper.

Conflicts of Interest: The authors declare no conflict of interest. The funders had no role in the design of this study, in the collection, analyses, or interpretation of the data, in the writing of the manuscript, or in the decision to publish the results.

References

1. Cook, B.I.; Mankin, J.S.; Anchukaitis, K.J. Climate Change and Drought: From Past to Future. *Curr. Clim. Chang. Rep.* **2018**, *4*, 164–179. [[CrossRef](#)]
2. Zhao, M.; Running, S.W. Drought-induced reduction in global terrestrial net primary production from 2000 through 2009. *Science* **2010**, *329*, 940–943. [[CrossRef](#)] [[PubMed](#)]
3. Kelley, C.P.; Mohtadi, S.; Cane, M.A.; Seager, R.; Kushnir, Y. Climate change in the Fertile Crescent and implications of the recent Syrian drought. *Proc. Natl. Acad. Sci. USA* **2015**, *112*, 3241–3246. [[CrossRef](#)]
4. Vicente-Serrano, S.M.; Gouveia, C.; Camarero, J.J.; Begueria, S.; Trigo, R.; Lopez-Moreno, J.I.; Azorin-Molina, C.; Pasho, E.; Lorenzo-Lacruz, J.; Revuelto, J.; et al. Response of vegetation to drought time-scales across global land biomes. *Proc. Natl. Acad. Sci. USA* **2013**, *110*, 52–57. [[CrossRef](#)]
5. Beloiu, M.; Stahlmann, R.; Beierkuhnlein, C. Drought impacts in forest canopy and deciduous tree saplings in Central European forests. *For. Ecol. Manag.* **2022**, *509*, 120075. [[CrossRef](#)]
6. Hossain, M.L.; Li, J. Biomass partitioning of C3- and C4-dominated grasslands in response to climatic variability and climate extremes. *Environ. Res. Lett.* **2021**, *16*, 074016. [[CrossRef](#)]
7. Torreño, A.A.; Barrera-González, J.; Lozano-Parra, J.; Garrido-Velarde, J. Assessment of Bare Soil in Extensive Livestock Areas in the Southwest of the Iberian Peninsula by Multi-Temporal Orthophotographs (2002–2016). In *Handbook of Research on Current Advances and Challenges of Borderlands, Migration, and Geopolitics*; IGI Global: Hershey, PA, USA, 2023; pp. 179–193.
8. Seager, R.; Ting, M.; Li, C.; Naik, N.; Cook, B.; Nakamura, J.; Liu, H. Projections of declining surface-water availability for the southwestern United States. *Nat. Clim. Chang.* **2012**, *3*, 482–486. [[CrossRef](#)]
9. Chen, J.; Dong, G.; Chen, J.; Jiang, S.; Qu, L.; Legesse, T.G.; Zhao, F.; Tong, Q.; Shao, C.; Han, X. Energy balance and partitioning over grasslands on the Mongolian Plateau. *Ecol. Indic.* **2022**, *135*, 108560. [[CrossRef](#)]
10. Doležal, J.; Altman, J.; Jandová, V.; Chytrý, M.; Conti, L.; Méndez-Castro, F.E.; Klimešová, J.; Zelený, D.; Ottaviani, G. Climate warming and extended droughts drive establishment and growth dynamics in temperate grassland plants. *Agric. For. Meteorol.* **2022**, *313*, 108762. [[CrossRef](#)]
11. Liu, H.; Lin, L.; Wang, H.; Zhang, Z.; Shangguan, Z.; Feng, X.; He, J.-S. Simulating warmer and drier climate increases root production but decreases root decomposition in an alpine grassland on the Tibetan plateau. *Plant Soil* **2020**, *458*, 59–73. [[CrossRef](#)]
12. Lei, T.; Wu, J.; Li, X.; Geng, G.; Shao, C.; Zhou, H.; Wang, Q.; Liu, L. A new framework for evaluating the impacts of drought on net primary productivity of grassland. *Sci. Total Environ.* **2015**, *536*, 161–172. [[CrossRef](#)]
13. Luo, W.; Zuo, X.; Griffin-Nolan, R.J.; Xu, C.; Ma, W.; Song, L.; Helsen, K.; Lin, Y.; Cai, J.; Yu, Q.; et al. Long term experimental drought alters community plant trait variation, not trait means, across three semiarid grasslands. *Plant Soil* **2019**, *442*, 343–353. [[CrossRef](#)]
14. Xu, C.; Ke, Y.; Zhou, W.; Luo, W.; Ma, W.; Song, L.; Smith, M.D.; Hoover, D.L.; Wilcox, K.R.; Fu, W.; et al. Resistance and resilience of a semi-arid grassland to multi-year extreme drought. *Ecol. Indic.* **2021**, *131*, 108139. [[CrossRef](#)]
15. Carroll, C.J.W.; Slette, I.J.; Griffin-Nolan, R.J.; Baur, L.E.; Hoffman, A.M.; Denton, E.M.; Gray, J.E.; Post, A.K.; Johnston, M.K.; Yu, Q.; et al. Is a drought a drought in grasslands? Productivity responses to different types of drought. *Oecologia* **2021**, *197*, 1017–1026. [[CrossRef](#)] [[PubMed](#)]
16. Lei, T.; Feng, J.; Lv, J.; Wang, J.; Song, H.; Song, W.; Gao, X. Net Primary Productivity Loss under different drought levels in different grassland ecosystems. *J. Environ. Manag.* **2020**, *274*, 111144. [[CrossRef](#)] [[PubMed](#)]
17. Isbell, F.; Craven, D.; Connolly, J.; Loreau, M.; Schmid, B.; Beierkuhnlein, C.; Bezemer, T.M.; Bonin, C.; Bruehlheide, H.; de Luca, E.; et al. Biodiversity increases the resistance of ecosystem productivity to climate extremes. *Nature* **2015**, *526*, 574–577. [[CrossRef](#)] [[PubMed](#)]
18. Li, L.; Zheng, Z.; Biederman, J.A.; Qian, R.; Ran, Q.; Zhang, B.; Xu, C.; Wang, F.; Zhou, S.; Che, R.; et al. Drought and heat wave impacts on grassland carbon cycling across hierarchical levels. *Plant Cell Environ.* **2021**, *44*, 2402–2413. [[CrossRef](#)]
19. Pimm, S.L. The complexity and stability of ecosystems. *Nature* **1984**, *307*, 321–326. [[CrossRef](#)]
20. Hossain, M.L.; Kabir, M.H.; Nila, M.U.S.; Rubaiyat, A. Response of grassland net primary productivity to dry and wet climatic events in four grassland types in Inner Mongolia. *Plant Environ. Interact.* **2021**, *2*, 250–262. [[CrossRef](#)]
21. Cui, A.; Li, J.; Zhou, Q.; Zhu, R.; Liu, H.; Wu, G.; Li, Q. Use of a multiscalar GRACE-based standardized terrestrial water storage index for assessing global hydrological droughts. *J. Hydrol.* **2021**, *603*, 126871. [[CrossRef](#)]
22. Liu, Y.; Zhu, Y.; Ren, L.; Singh, V.P.; Yang, X.; Yuan, F. A multiscalar Palmer drought severity index. *Geophys. Res. Lett.* **2017**, *44*, 6850–6858. [[CrossRef](#)]
23. Vicente-Serrano, S.M.; Beguería, S.; López-Moreno, J.I.; Angulo, M.; El Kenawy, A. A New Global 0.5° Gridded Dataset (1901–2006) of a Multiscalar Drought Index: Comparison with Current Drought Index Datasets Based on the Palmer Drought Severity Index. *J. Hydrometeorol.* **2010**, *11*, 1033–1043. [[CrossRef](#)]
24. Begueria, S.; Vicente-Serrano, S.M.; Reig, F.; Latorre, B. Standardized precipitation evapotranspiration index (SPEI) revisited: Parameter fitting, evapotranspiration models, tools, datasets and drought monitoring. *Int. J. Climatol.* **2014**, *34*, 3001–3023. [[CrossRef](#)]
25. Anderegg, W.R.L.; Trugman, A.T.; Badgley, G.; Konings, A.G.; Shaw, J. Divergent forest sensitivity to repeated extreme droughts. *Nat. Clim. Chang.* **2020**, *10*, 1091–1119. [[CrossRef](#)]
26. Deng, Y.; Wu, D.; Wang, X.; Xie, Z. Responding time scales of vegetation production to extreme droughts over China. *Ecol. Indic.* **2022**, *136*, 108630. [[CrossRef](#)]

27. Deng, L.; Shangguan, Z.-P.; Wu, G.-L.; Chang, X.-F. Effects of grazing exclusion on carbon sequestration in China's grassland. *Earth-Sci. Rev.* **2017**, *173*, 84–95. [CrossRef]
28. Wang, S.; Tuya, H.; Zhang, S.; Zhao, X.; Liu, Z.; Li, R.; Lin, X. Random forest method for analysis of remote sensing inversion of aboveground biomass and grazing intensity of grasslands in Inner Mongolia, China. *Int. J. Remote Sens.* **2023**, *44*, 2867–2884. [CrossRef]
29. National Forestry and Grassland Administration. In China, 40% of the Land Is Grassland. Available online: <http://www.forestry.gov.cn/main/5462/20210311/115701724435306.html> (accessed on 1 September 2023).
30. Wang, X.; Luo, P.; Zheng, Y.; Duan, W.; Wang, S.; Zhu, W.; Zhang, Y.; Nover, D. Drought Disasters in China from 1991 to 2018: Analysis of Spatiotemporal Trends and Characteristics. *Remote Sens.* **2023**, *15*, 1708. [CrossRef]
31. Wang, Y.; Liu, G.; Guo, E. Spatial distribution and temporal variation of drought in Inner Mongolia during 1901–2014 using Standardized Precipitation Evapotranspiration Index. *Sci. Total Environ.* **2019**, *654*, 850–862. [CrossRef]
32. Huang, K.; Xia, J. High ecosystem stability of evergreen broadleaf forests under severe droughts. *Glob. Chang. Biol.* **2019**, *25*, 3494–3503. [CrossRef]
33. Vicente-Serrano, S.M.; Beguería, S.; López-Moreno, J.I. A Multiscalar Drought Index Sensitive to Global Warming: The Standardized Precipitation Evapotranspiration Index. *J. Clim.* **2010**, *23*, 1696–1718. [CrossRef]
34. Dorman, M.; Svoray, T.; Perevolotsky, A.; Sarris, D. Forest performance during two consecutive drought periods: Diverging long-term trends and short-term responses along a climatic gradient. *For. Ecol. Manag.* **2013**, *310*, 1–9. [CrossRef]
35. Xu, P.; Fang, W.; Zhou, T.; Li, H.; Zhao, X.; Berman, S.; Zhang, T.; Yi, C. Satellite evidence of canopy-height dependence of forest drought resistance in southwestern China. *Environ. Res. Lett.* **2022**, *17*, 025005. [CrossRef]
36. IPCC. *Climate Change 2021*; Cambridge University Press: Cambridge, UK, 2021.
37. An, Q.; He, H.; Nie, Q.; Cui, Y.; Gao, J.; Wei, C.; Xie, X.; You, J. Spatial and Temporal Variations of Drought in Inner Mongolia, China. *Water* **2020**, *12*, 1715. [CrossRef]
38. Liang, M.; Cao, R.; Di, K.; Han, D.; Hu, Z. Vegetation resistance and resilience to a decade-long dry period in the temperate grasslands in China. *Ecol. Evol.* **2021**, *11*, 10582–10589. [CrossRef]
39. Miao, Y.; Zhou, Z.; Jiang, M.; Song, H.; Yan, X.; Liu, P.; Ji, M.; Han, S.; Chen, A.; Wang, D. Resistance and Resilience of Nine Plant Species to Drought in Inner Mongolia Temperate Grasslands of Northern China. *Appl. Sci.* **2022**, *12*, 4967. [CrossRef]
40. Hossain, M.L.; Li, J. NDVI-based vegetation dynamics and its resistance and resilience to different intensities of climatic events. *Glob. Ecol. Conserv.* **2021**, *30*, e01768. [CrossRef]
41. Ma, W.; Liang, X.; Wang, Z.; Luo, W.; Yu, Q.; Han, X. Resistance of steppe communities to extreme drought in northeast China. *Plant Soil* **2022**, *473*, 181–194. [CrossRef]
42. Zhang, L.H.; Wang, J.F.; Zhao, R.F.; Guo, Y.F.; Hao, L.Y.; Hu, Z.M. Aboveground net primary productivity and soil respiration display different responses to precipitation changes in desert grassland. *J. Plant Ecol.* **2022**, *15*, 57–70. [CrossRef]
43. Mackie, K.A.; Zeiter, M.; Bloor, J.M.G.; Stampfli, A. Plant functional groups mediate drought resistance and recovery in a multisite grassland experiment. *J. Ecol.* **2019**, *107*, 937–949. [CrossRef]
44. Cleland, E.E.; Chiariello, N.R.; Loarie, S.R.; Mooney, H.A.; Field, C.B. Diverse responses of phenology to global changes in a grassland ecosystem. *Proc. Natl. Acad. Sci. USA* **2006**, *103*, 13740–13744. [CrossRef] [PubMed]
45. Guo, J.W.; Zhao, C.C.; Zhang, L.N.; Han, Y.Y.; Cao, R.; Liu, Y.Z.; Sun, S.C. Water table decline alters arthropod community structure by shifting plant communities and leaf nutrients in a Tibetan peatland. *Sci. Total Environ.* **2022**, *814*, 151944. [CrossRef] [PubMed]
46. Stuart-Haentjens, E.; De Boeck, H.J.; Lemoine, N.P.; Mand, P.; Kroel-Dulay, G.; Schmidt, I.K.; Jentsch, A.; Stampfli, A.; Anderegg, W.R.L.; Bahn, M.; et al. Mean annual precipitation predicts primary production resistance and resilience to extreme drought. *Sci. Total Environ.* **2018**, *636*, 360–366. [CrossRef]
47. Zhong, M.X.; Song, J.; Zhou, Z.X.; Ru, J.Y.; Zheng, M.M.; Li, Y.; Hui, D.F.; Wan, S.Q. Asymmetric responses of plant community structure and composition to precipitation variabilities in a semi-arid steppe. *Oecologia* **2019**, *191*, 697–708. [CrossRef] [PubMed]
48. Knapp, A.K.; Carroll, C.J.; Denton, E.M.; La Pierre, K.J.; Collins, S.L.; Smith, M.D. Differential sensitivity to regional-scale drought in six central US grasslands. *Oecologia* **2015**, *177*, 949–957. [CrossRef]
49. Vandeger, R.K.; Tissue, D.T.; Hartley, S.E.; Glauser, G.; Johnson, S.N. Physiological acclimation of a grass species occurs during sustained but not repeated drought events. *Environ. Exp. Bot.* **2020**, *171*, 103954. [CrossRef]
50. Tielborger, K.; Bilton, M.C.; Metz, J.; Kigel, J.; Holzapfel, C.; Lebrija-Trejos, E.; Konsens, I.; Parag, H.A.; Sternberg, M. Middle-Eastern plant communities tolerate 9 years of drought in a multi-site climate manipulation experiment. *Nat. Commun.* **2014**, *5*, 5102. [CrossRef]

Disclaimer/Publisher's Note: The statements, opinions and data contained in all publications are solely those of the individual author(s) and contributor(s) and not of MDPI and/or the editor(s). MDPI and/or the editor(s) disclaim responsibility for any injury to people or property resulting from any ideas, methods, instructions or products referred to in the content.